Science of the Total Environment 643 (2018) 1127–1136

Contents lists available at ScienceDirect

Science of the Total Environment

journal homepage: www.elsevier.com/locate/scitotenv

Comparing anthropogenic heat input and heat accumulation in the subsurface of Osaka, Japan

Susanne A. Benz [a,b,*], Peter Bayer [c], Philipp Blum [b], Hideki Hamamoto [d], Hirotaka Arimoto [e], Makoto Taniguchi [a]

[a] Research Institute for Humanity and Nature (RIHN), Kyoto, Japan
[b] Institute of Applied Geosciences (AGW), Karlsruhe Institute of Technology (KIT), Karlsruhe, Germany
[c] Institute of new Energy Systems (InES), Ingolstadt University of Applied Sciences, Ingolstadt, Germany
[d] Center for Environmental Science in Saitama, Saitama, Japan
[e] Geo-Research Institute, Osaka, Japan

HIGHLIGHTS

- Heat flux into the underground is quantified for 4 heat sources and 15 wells.
- Heat flux in Osaka is considerably lower than previously determined flux in Europe.
- Sealed surfaces and buildings contribute equally to urban subsurface warming.
- Temporal analysis reveals little variation in annual heat input.
- For undisturbed wells heat accumulation correlates to heat input, but is lower.

GRAPHICAL ABSTRACT

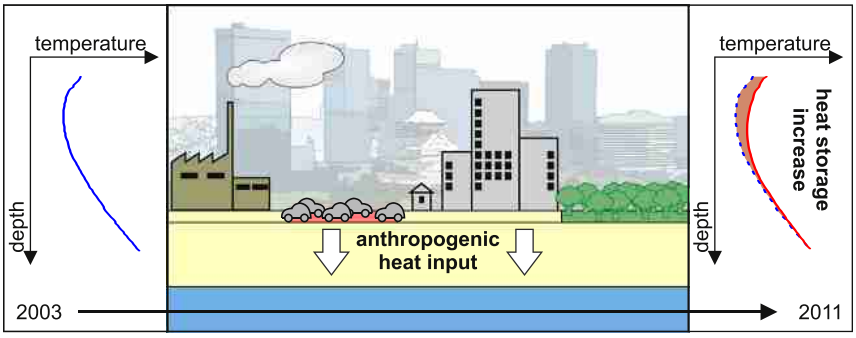

ARTICLE INFO

Article history:
Received 1 May 2018
Received in revised form 19 June 2018
Accepted 20 June 2018
Available online xxxx

Editor: José Virgílio Cruz

Keywords:
Urban heat islands
Subsurface urban heat islands
Groundwater temperatures
Anthropogenic heat flux
Heat recycling
Geothermal potential

ABSTRACT

In metropolitan areas, shallow groundwater temperatures are affected by anthropogenic heat sources. The resulting thermal conditions in the subsurface are highly site-specific, and spatial and temporal trends have only been revealed for a few cities. In this study, the anthropogenic heat input is quantified for 15 locations in Osaka, Japan using an analytical, one-dimensional conductive heat transport model. Mean anthropogenic fluxes into the subsurface are determined annually between 2003 and 2011. The model depicts fluxes from buildings and from different land cover types separately. The main objective is to compare the predicted annual mean heat input to heat storage increase, and to identify site-specific factors relevant for the thermal evolution of the underground at each well location. Our results indicate that mean fluxes from asphalt covered areas (0.28 ± 0.07 W/m^2) and from buildings (0.32 ± 0.18 W/m^2) are significantly higher than fluxes from unpaved (0.06 ± 0.06 W/m^2) and grass-covered (-0.04 ± 0.06 W/m^2) areas. Furthermore, the temporal variation of mean fluxes from buildings is stable over the studied time period, while annual mean fluxes from asphalt, grass and unpaved areas vary as much as 0.8 MJ/m^2. Still, the uncertainty associated with the combined annual heat input of all heat sources is slightly higher than the changes between the years. Overall, the predicted cumulative heat input (2003 to 2011) at the wells ranges from 4 MJ/m^2 to 60 MJ/m^2. Comparing these results to heat storage increase, additional local heat fluxes, such as from construction work or a sewage treatment plant, have to be considered for about 1/3 of the wells. In addition, it becomes apparent that a significant percentage of determined anthropogenic heat input is not stored in the urban aquifer and heat input is predicted to be considerably higher than heat storage increase.

* Corresponding author at: Research Institute for Humanity and Nature (RIHN), Kyoto, Japan.
E-mail address: susanne.benz@kit.edu (S.A. Benz).

https://doi.org/10.1016/j.scitotenv.2018.06.253
0048-9697/

1. Introduction

Today >50% of humanity lives within an urban environment (United Nations, 2015). Here temperatures are commonly elevated compared to the rural background (Oke, 1973). These resulting urban heat islands (UHI) are primarily a concern in the atmosphere, where they have far reaching and mainly negative implications on human health (Patz et al., 2005; Vandentorren et al., 2006) and energy consumption (Ewing and Rong, 2008; Kolokotroni et al., 2006; Santamouris, 2014). Moreover, they are also present in the underlying aquifers (Attard et al., 2016; Bucci et al., 2017; Epting and Huggenberger, 2013; Ferguson and Woodbury, 2004, 2007; Huang et al., 2009; Menberg et al., 2013a; Müller et al., 2014; Taniguchi et al., 2007; Taniguchi et al., 2009; Yalcin and Yetemen, 2009). In fact, in many cities, urban heat islands appear to be more pronounced in the subsurface than in the atmosphere and at the surface (Benz et al., 2016; Benz et al., 2017b).

A main motivation for exploring the thermal conditions beneath cities is the growing interest in geothermal energy (Arola and Korkka-Niemi, 2014; Benz et al., 2015; Epting et al., 2017; García-Gil et al., 2014; Mueller et al., 2018). In Europe, in the USA, and in Japan, 80%, 60%, and approximately 50% of the residential energy consumption is used for water and space heating (Eurostat, 2017; Komiyama and Marnay, 2008; U.S. Energy Information Administration (EIA), 2012). Decarbonizing this energy would lead to an overall improvement of the sustainability of our current energy management. For instance, a study in California found that decarbonizing water heating alone could result in savings of over 10 million tons of annual greenhouse gas emission (Raghavan et al., 2017). One way to decarbonize heating is through the use of shallow geothermal energy. Shallow geothermal applications such as groundwater heat pump (GWHP) systems and ground source heat pump (GSHP) systems, usually equipped with vertical borehole heat exchangers (BHE), are expected to increase in numbers worldwide (Bayer et al., 2012). In subsurface urban heat islands (SUHI), an increased geothermal potential for utilizing the shallow urban ground and groundwater for heating purposes is reported (Allen et al., 2003; Farr et al., 2017; Herbert et al., 2013; Rivera et al., 2017; Zhu et al., 2010). As geothermal systems are applied for decades, the local thermal evolution in the subsurface is of major interest for these commonly small scale applications. So far, however, there is little known about the annual variations of anthropogenic heat fluxes into the subsurface and their long-term effects on the thermal conditions of the urban underground.

Local effects in urban settings are often examined for individual borehole temperature profiles (Colombani et al., 2016; Dettwiller, 1970; Reiter, 2006; Westaway et al., 2015) and were captured in two- or three-dimensional borehole temperature models by Dědeček et al. (2012) and Bayer et al. (2016). City-wide analyses were previously performed especially for central European cities such as Karlsruhe and Cologne in Germany, and Basel in Switzerland (Benz et al., 2015; Epting and Huggenberger, 2013; Menberg et al., 2013b; Mueller et al., 2018). Menberg et al. (2013b) compared the conditions observed in recent city-wide groundwater measurements in Karlsruhe to those from the 1970s to identify general trends, and Mueller et al. (2018) set up a three-dimensional (3D) groundwater flow and heat transport model to assess the potentially usable shallow geothermal energy in Basel. However, previous studies have not focused on the annual variation of temperatures and heat fluxes at local observation wells.

In general, there are two basic ways to investigate the evolution of the thermal regime around a borehole as well as the role of potential heat sources: Either a single temperature profile is logged and reproduced by a calibrated heat transport model, or temperature profiles taken at different times are compared. While simplified assumptions can be made for the governing processes, meaningful results from single temperature logs can only be achieved when the physical ground properties are well known. This is commonly feasible with one-dimensional conduction (and advection) models which are mainly used in borehole climatology to reconstruct ground surface temperature history (Bodri and Cermak, 2011; Goto et al., 2005; Kurylyk et al., 2014; Kurylyk and MacQuarrie, 2014). These may also be suitable to infer the onset of urbanization (Taniguchi et al., 2007), and to quantify the contributions from different heat sources and processes. However, as shown for example by Colombani et al. (2016), the superpositioning of multiple effects renders it often impossible to distinguish their individual contributions and thus to predict the evolution of anthropogenic heat fluxes.

To explore, the long-term behavior of the groundwater thermal regime, repeated profiles should ideally be taken with at least several years between measurements (Bense et al., 2017; Bense and Kurylyk, 2017; Ferguson and Woodbury, 2007). The study by Cermak et al. (2017) reports accelerated heat flux through artificial land covers such as asphalted ground, which is based on eleven years of monitoring of the upper 50 cm beneath different land cover types. Kooi (2008) examined borehole temperature profiles in 16 wells in the Netherlands, which had been measured again after around three decades. This study revealed the crucial insight obtained from repeated measurement to estimate the role of different site characteristics, groundwater effects and land use changes, but similar to the work by Šafanda et al. (2007) in other European countries, the role of urban conditions was not in the foreground. In contrast, Yamano et al. (2009) presented profiles recorded within around two years in a selected well of Taipei, and repeated measurements between 1993 and 2006 from another well close to a museum 50 km NE of Osaka. As a consequence of permanent heat loss from the building of this museum, a nearly linear increase of the ground temperature was observed. Ferguson and Woodbury (2007) investigated trends in wells in Winnipeg measured in 2002 and 2007, and a qualitative explanation of observed temperature changes in some wells was presented. Warming trends were interpreted by heat release from a re-occupied building and by enhanced heat injection, and as potential causes of local cooling, demolishing of a building and changes in the ambient groundwater flow regime were proposed. A quantitative analysis however is missing.

In the present study, the annual anthropogenic heat input into the shallow urban aquifer beneath Osaka, Japan is quantified based on well temperature logs from 2003 and 2011. Fluxes from different land cover types and buildings are analyzed separately in order to better understand the concerted influence of individual heat sources on the prevailing subsurface urban heat island over the years. The main objective is to compare the heat fluxes predicted from a one-dimensional (1D) conduction model to the heat storage increase. This comparison will ideally enable model evaluation and identification of site-specific factors relevant for the thermal evolution around monitoring wells.

2. Materials and methods

2.1. Study area

Osaka is the third largest city of Japan and located at Osaka Bay west of the Seto Inland Sea. While the city itself has a population of 2.7 million, it is part of the Keihanshin city cluster with Kyoto and Kobe hosting a total population of close to 20 million. Osaka is located in a temperate climate with hot summers and no dry season (Peel et al., 2007). The upper layer of the urban underground consists of alternating layers of sands, gravels, clay and silts (Fig. S1) with a thickness of 30 to 50 m. A more detailed insight into the geological setting of Osaka can be found in Mitamura et al. (1994) and in reports from the Kansai Geoinformatic Network (KG-NET, 2007). Groundwater depth ranges from 4 to 14 m below ground (Figs. A1 and S2) with complex but slow groundwater flow, mainly in the direction of the river delta at Osaka Bay. A detailed map of the local hydrological conditions is available online from the Japan Ministry of Land, Infrastructure, Transport and Tourism, Land and Water Bureau, National Land Survey Division (2018).

Several groundwater observation wells in the city are managed by the municipality in order to collect additional information on ground subsidence, which was observed from the early 1930s onward due to excessive groundwater pumping. After regulations, subsidence declined and groundwater levels in the Osaka plain are now rather stable (Mitamura et al., 1994; Taniguchi and Uemura, 2005). In the year 2003, temperatures in 34 boreholes were measured by Taniguchi and Uemura (2005) in 1 m vertical intervals and again by Arimoto et al. (2015) in 2011. Here, those 15 wells are analyzed that are deep enough (~60 m) to capture the entire increase in heat storage and that have a groundwater depth ≤ 20 m (Fig. 1). For consistency, the nomenclature from Taniguchi and Uemura (2005) is adopted. In their study, they discussed the impact of vertical groundwater flux and temperature change of the last 120 years on selected borehole temperature profiles. They found that warming due to urbanization had occurred earlier within the city center than in the surrounding areas. Since they observed seasonal variation in temperatures down to 18 m, we chose 20 m depth as the reference level for this study. This means that focus is set on the long term thermal evolution of groundwater below a depth of 20 m.

2.2. Anthropogenic heat input

2.2.1. Methodology

In this study, the cumulative anthropogenic heat input into the underground is quantified at each well location for four different heat sources: heat from (1) buildings, heat from surfaces covered by (2) asphalt, (3) sand and bare soil, and (4) grass. Fluxes from elevated surface temperatures and buildings were previously determined as dominant on a city-wide scale (Benz et al., 2015, 2016; Menberg et al., 2013b). Hence, heat sources found to be minor by these studies, such as the sewage system, are not considered here. The effect from underground structures is also not accounted for, because such structures are not present near any of the wells and residential buildings in Osaka typically have no basement.

Overall the procedure consists of three steps: First, the annual mean heat flux q_j^i is quantified for each year i and each heat source j; next, the combined annual heat input Q_I^i of all heat sources is determined for each year; finally, they are added up to give the cumulative heat input Q_I between 2003 and 2011.

2.2.1.1. Heat flux. Annual mean, vertical heat flux is quantified with a 1D, statistical, analytical heat flux model based on the models introduced by Menberg et al. (2013b) and Benz et al. (2015). It uses a Monte Carlo approach here: 800 iterations following Benz et al. (2015) to represent the uncertainty and natural range of all input parameters. It is formulated to quantify heat fluxes to the reference level $D = 20$ m depth at the 15 selected well locations, considering the different lithological layers and building insulation.

The analyzed four types of heat input are by conduction and annual mean fluxes [W/m^2] are therefore quantified by Fourier's law:

$$q_j^i = \lambda_j^i \cdot \frac{T_j^i - T_{GW}^i}{D} \quad (1)$$

T_{GW}^i is the groundwater temperature at 20 m depth for each year i, T_j^i is the temperature of each heat source j, here building or surface (asphalt, sand, or grass) temperature, and λ_j^i is the thermal conductivity between the heat source and $D = 20$ m.

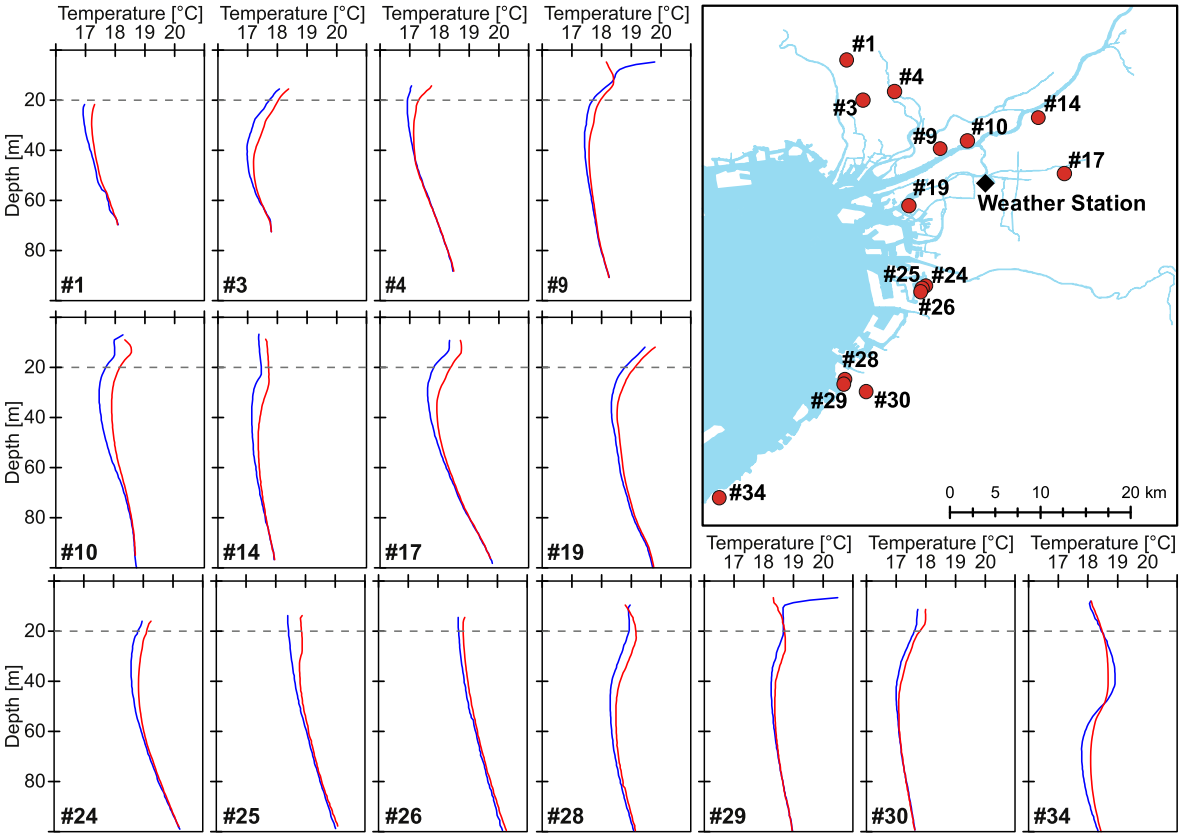

Fig. 1. Map of all wells and the weather station in Osaka, and corresponding groundwater temperatures in 2003 (blue) and 2011 (red). In well #1 temperatures were only measured below a depth of around 21 m. Dashed lines denote the depth of 20 m taken as reference level in this study. (For interpretation of the references to color in this figure legend, the reader is referred to the web version of this article.)

2.2.1.2. Annual heat input. The annual heat input Q_I^i [MJ/m^2] of each year i is a combination of fluxes q_j^i of the individual heat sources j and depends on the land cover density (e.g. asphalted area per surface area) or building density (area of building per surface area) ρ_j^i around each well:

$$Q_I^i = \sum \rho_j^i \cdot q_j^i \quad (2)$$

2.2.1.3. Cumulative heat input. To determine the cumulative anthropogenic heat input Q_I [MJ/m^2] between 2003 and 2011, the annual heat inputs of the individual years are added up:

$$Q_I = \sum_{i=2003}^{2010} Q_I^i \quad (3)$$

2.2.2. Model parameter values

All parameter values except measured groundwater temperature and depth are considered uncertain and therefore varied within a Monte Carlo analysis assuming a triangular distribution defined by minimum, mode and maximum values.

2.2.2.1. Thermal conductivity. When quantifying fluxes from the different surface cover types (sand and bare soil, asphalt, and grass), the thermal conductivity of the underground down to 20 m depth is approximated by the thickness-weighted harmonic mean of the thermal conductivities of the individual lithological layers (Fig. S1, Table 1). As site-specific values are not available, thermal conductivity was taken from the VDI (2010). To account for the associated uncertainties, mode values were set to each characteristic value, and the given range is used as minimum and maximum. We distinguish unsaturated and saturated layers, which differ each year depending on the water table. For the unsaturated zone median values of saturated and dry media were taken into account for each of the analyzed facies. Since the water table was only measured in 2003 and 2011 (Fig. S2), assuming constant boundary conditions, a linear change between these years was assumed (Fig. A1).

For computing heat release from buildings, the underfloor of the structure has to be considered. Following the Building Standard Law – Construction Order, Article 22 of Japan, the underfloor of a building has be at least 0.45 m of space or concrete (Hasegawa, 2013). Hence, the modelled top 0.45 m of the ground are replaced by underfloor in the simulated lithological columns (Fig. S1), and based on this the harmonic mean is determined. For the assumed thermal conductivity of the underfloor, values were set as follows: minimum of 0.02 W/mK (representing an air filled underfloor); mode of 0.16 W/mK (concrete with 10 cm glass wool insulation); maximum of 1.6 W/mK (concrete without insulation) (VDI, 2010).

2.2.2.2. Surface and building temperatures. To quantify fluxes from buildings, temperatures of the lowest floor are taken as reference. In Osaka these rooms are commonly equipped with air conditioning devices. Hence, annual mean room temperature according to the "Technical standards concerning maintenance and cleaning of air conditioning equipment, etc." established by the Ministry of Health, Labor and Welfare, Japan are set as model parameter values: minimum of 17 °C; mode of 22.5 °C; and maximum of 28 °C. Building temperatures are assumed to be independent of outside temperatures and are not varied for different years.

For the different land cover types, ground surface temperatures are needed to quantify heat flux into the subsurface. They are estimated by adding a land cover dependent offset ΔT to a background air temperature. Offsets ΔT were measured by Dědeček et al. (2012) for asphalt (min: 4.0 K; mode: 4.5 K; max: 5.0 K), sand and bare soil (min: 1.0 K; mode: 1.75 K; max: 2.0 K), and grass (min: 0.2 K; mode: 0.5 K; max: 0.8 K). These values were also previously used by Benz et al. (2015) to estimate ground surface temperatures and differences between the individual land covers agree with results from a ground surface temperature simulation by Herb et al. (2008). Air temperatures in central Osaka are observed by the Japan Meteorological Agency (Fig. 1). Fig. A1 shows annual mean air temperatures from 2003 to 2011.

2.2.2.3. Groundwater temperatures. As descripted in Section 2.1. *Study Area*, groundwater temperatures were measured in 2003 and in 2011 (Fig. S2). Assuming constant thermal boundary conditions, a logarithmic temperature change between these years was assumed for the reference depth of 20 m (Fig. A1).

2.2.2.4. Land cover densities and building density. For each well, the surrounding land cover types and buildings are given in Fig. 2. Buildings, water ways and the sea, green areas (such as parks and gardens), and asphalt covered locations (such as streets and parking lots) were extracted from open street maps and updated manually from the satellite imagery of Google maps. The background is considered sand and bare soil. For two wells, land cover changed during the analyzed timeframe. East of well #10 a building was constructed in 2007 and some areas were paved that were previously bare. Also, major construction work began in 2007 just south of well #25; it was not completed by the end of the analyzed period in 2011. While we were unable to identify the nature of this construction work, satellite imagery reveals the construction of several temporary warehouses and implies the existence of a deep excavation. Within the model, this unfinished construction is described as a land cover change from grass to bare soil.

Land cover and building densities were determined for the areas surrounding each well. In our 1D conductive heat flux model, the radius of this area is varied within the Monte Carlo approach from 1 to 100 m (Fig. S3) to account for the expected range, caused for example by different lithology and by the geometry of heat sources on the surface. The radius of 100 m was chosen as a maximum distance as this is the approximate extent of the thermally affected zone of an underground structure (Attard et al., 2016). Heat sources outside of this radius are therefore unlikely to have a significant impact on heat storage increase at the well location. Hence, building density and land cover density were determined for all possible areas with a radius of up to 100 m (1 m steps, Fig. 2). While densities for most wells are independent of time, the above mentioned land cover changes around wells #10 and #25 yielded a local change in land use density since 2007 for these two wells. Areas covered by water are not considered in our conductive heat flux model, but heat transport through advection is expected at these boundaries.

Table 1
Values for the thermal conductivity of the unsaturated zone (λ_{unsat}) and of the aquifer ($\lambda_{aquifer}$) used in the heat input model as well values for the heat capacity C_V used to quantify the increase in heat storage. The lithology of each well is depicted in Fig. S1.

	λ_{unsat} [W/mK][a]			$\lambda_{aquifer}$ [W/mK][a]			C_V [MJ/m^{3}K][a]	
	Min	Mode	Max	Min	Mode	Max	Min	Max
Sand	1.0	1.4	1.9	2.0	2.4	3.0	2.2	2.8
Gravel	0.9	1.1	1.7	1.6	1.8	2.5	2.2	2.6
Silt or clay	0.7	1.1	2.0	1.1	1.8	3.1	2.0	2.8
Silt or clay mixed with sand	0.8	1.2	1.9	1.6	2.1	3.0	2.1	2.8

[a] VDI 4640 (2010).

2.3. Increase in heat storage

The increase in heat storage Q_S between 2003 and 2011 below a depth of $D = 20\ m$ is determined for all wells. The maximum depth was set to 100 m below ground.

$$Q_S = \int_{D=20\ m}^{100\ m} C_V(D)\ (T_{2011}(D) - T_{2003}(D))\ dD \quad (4)$$

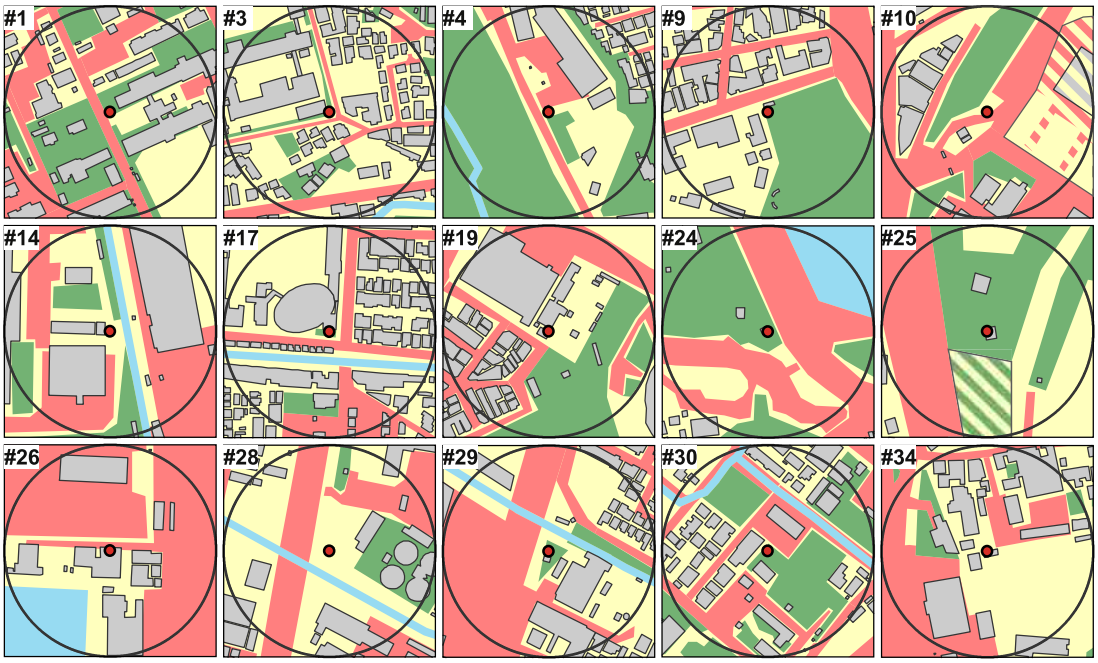

Fig. 2. Buildings (grey) and land cover around all well locations (red dot). Land covered by asphalt such as streets or parking lots are depicted in red, land covered by grass is green and water is given in blue. Within this study buildings and land cover types within a radius of up to of 100 m (black circle) are considered. For wells #10 and #25 areas affected by the land cover changes in 2007 are framed with a thin grey line and shown in striped colors. (For interpretation of the references to color in this figure legend, the reader is referred to the web version of this article.)

Here $T_{2011}(D)$ and $T_{2003}(D)$ are groundwater temperature depth profiles measured in 2011 and 2003 in steps of 1 m respectively (Fig. 1), and $C_V(D)$ is the heat capacity at any given depth D. It is derived from the lithology of each well (Fig. S1) using values given in Table 1. As all wells apart from well #34 are within a single aquifer, only saturated media were assumed. Still, there is a natural range within the heat capacity of certain media (here represented by maximum and minimum values), and a Monte Carlo approach (uniform distribution of heat capacity) with 800 iterations was used.

3. Results and discussion

3.1. Heat flux

Fig. 3 shows heat flux from (1) buildings and fluxes from surfaces covered by (2) asphalt, (3) sand and bare soil, and (4) grass for all wells (Eq. (1)). Mean values are provided in Table A1. In agreement with previous findings (Benz et al., 2015; Menberg et al., 2013b), buildings reveal to be the most dominant source of heat flux with on average 0.32 ± 0.18 W/m^2. In comparison, studies in Europe found much higher fluxes of 3.61 ± 3.37 W/m^2 in Karlsruhe, Germany, 0.57 ± 0.25 W/m^2 in Cologne, Germany (Benz et al., 2015) and 5.9 to 8.0 W/m^2 in Basel, Switzerland (Mueller et al., 2018). The different results can mainly be attributed to different insulation and temperatures of buildings, and a lack of basements within Osaka, resulting in a greater distance between groundwater and building and therefore a lower thermal gradient.

The second most relevant energy flux originates from paved surfaces. With a mean value of 0.28 ± 0.07 W/m^2 it reaches about 87% of the fluxes from buildings, but with a significantly lower standard deviation. This can be attributed to the uncertainties and ranges associated with building temperature (17 °C to 28 °C) and insulation. We can therefore expect that in areas with modern housing and better insulation, flux from asphalt exceeds the heat flux from buildings, at least in the absence of basements. Accordingly, a study carried out in the area

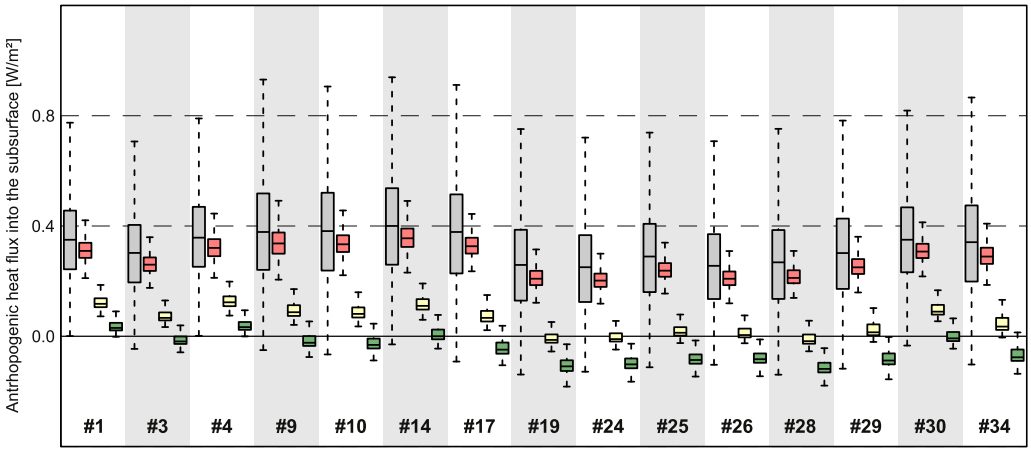

Fig. 3. Anthropogenic heat flux into the subsurface (Eq. (1)) at the well locations for flux from buildings (grey) and flux from the surface covered by asphalt (red), by sand or bare soil (yellow), and by grass (green). The black lines in the boxplot indicate median values, the bars correspond to the inner quartile range (IQR) ranging from the 25th percentile (p_{25}) to the 75th percentile (p_{75}). Whiskers span from the lowest value higher than $p_{25} - 1.5 \cdot IQR$ to the highest value lower than $p_{75} + 1.5 \cdot IQR$. (For interpretation of the references to color in this figure legend, the reader is referred to the web version of this article.)

of Zurich, Switzerland, identified asphalt as the dominating driver of subsurface temperatures in one well and buildings and asphalt to be of equal importance at another well (Bayer et al., 2016).

Mean heat fluxes from sand and bare soil are 0.06 ± 0.06 W/m^2 and fluxes from grass covered land are −0.04 ± 0.06 W/m^2. Overall mean flux from grass is negative for ten out of the 15 analyzed wells with the lowest value of −0.11 ± 0.03 W/m^2 at well #28 where ground water temperatures are highest. This indicates that, within urban green spaces, the SUHI is contributing to the surface urban heat island. Similar, however only qualitative, observations were previously made in Germany (Benz et al., 2015). Still, this impact of green spaces is most likely marginal as anthropogenic heat flux feeding atmospheric heat islands is commonly between 10 and 50 W/m^2 (Arnfield, 2003), and thus orders of magnitudes higher. A study set in Tokyo even identified fluxes as high as 1590 W/m^2 in daytime in winter (Ichinose et al., 1999).

Because previous studies did not quantify heat flux into the subsurface from different land cover types individually, results are difficult to compare. Within Germany, flux from the surface regardless of land cover type was determined to be 0.24 ± 0.11 W/m^2 in Karlsruhe and 0.21 ± 0.06 W/m^2 in Cologne (Benz et al., 2015). These values are comparable with the fluxes from asphalt in Osaka. This can be attributed to a slightly higher thermal gradient in Germany than in Osaka, caused by higher groundwater temperatures and a deeper reference level D = 20 m in Japan.

When comparing the individual wells, fluxes at wells #9, #10, and #14 are highest (Table A1). All these wells are located in the northeastern part of the city within 700 m of the Yodo River (Fig. 1). The high fluxes are caused by comparably low groundwater temperatures and a high water table (Figs. A1 and S2). Since groundwater flow is in general towards Osaka bay and the city center along the river, these relative low temperatures are likely influenced in part by inflowing groundwater from the less densely populated suburbs.

3.2. Annual heat input

Results for the combined annual heat input (Eq. (2)) as well as annual heat input of the individual heat sources are given in Figs. 4, S4 and Table S1. The mean combined annual heat input of all wells ranges from 4.0 ± 2.7 MJ/m^2 in 2006 and 2008 to 5.9 ± 2.6 MJ/m^2 in 2003. In comparison, the annual demand for space and water heating of the Japanese residential sector is roughly about 1200 PJ in total or <10 GJ per person (Komiyama and Marnay, 2008). Accordingly, the annual anthropogenic heat input into Osaka's groundwater (12,000 persons per km^2) could be sufficient to sustainably cover between 3 and 5% of the heating demand. In comparison, the sustainable geothermal potential for space heating in Karlsruhe and Cologne, Germany, is 32% and 9%, respectively (Benz et al., 2015), due to lower population density and higher heat fluxes. However, heating and cooling degree days in Osaka, which quantify the need for space heating and cooling from outside temperatures, are similar (Sivak, 2009). If cooling demand was to be covered with groundwater systems, anthropogenic heat input and therefore the sustainable geothermal potential for heating would increase notably. Still, it must be noted that the heating demand is highest for cold years, and this is when heat input from the surface into groundwater is lowest.

Highest annual heat input is determined for wells #17 and #14 (Table S1). These, together with wells #9 and #10, also show some of the highest heat fluxes (Fig. 3). However, building density at wells #17 and #14 is considerably higher than at wells #9 and #10 leading to an overall higher annual heat input. Lowest annual heat input is determined for well #25 with an average of only 0.4 ± 2.4 MJ/m^2 per year. This well has the highest fraction of grass cover surrounding it of all locations. Additionally, wells #10 and #25 experienced close by land cover changes in 2007 (Figs. 2 and S3). Near well #10, a building was constructed on a previously unpaved area and some locations were paved. Still, these land cover changes show little effect on annual heat input, and mean values even decrease from 5.8 ± 1.4 MJ/m^2 before 2007 to 5.6 ± 1.3 MJ/m^2 afterwards due to the unusually high surface temperatures in 2004 (Figs. A1 and S4). Similarly, the land use changes south of well #25 have little effect on annual heat input, and mean values also decrease (from 0.5 ± 2.5 MJ/m^2 to 0.4 ± 2.3 MJ/m^2) (Fig. S4). While a much larger area is affected here than at well #10, decreasing heat output due to loss of green space is counteracted by increasing groundwater temperatures making the remaining grass covered area more impactful on the combined annual heat input. Because heat flux from sand is approximately zero at this location (Fig. S3), increasing sand cover does not affect the heat input significantly.

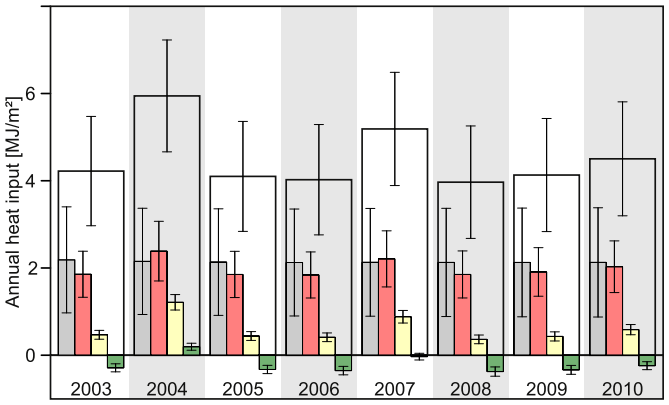

Fig. 4. Mean annual heat input (Eq. (2)) of all wells for the studied time period. Shown are the total heat input in form of a clear bar and in color the individual components: heat input from buildings (grey), asphalt (red), sand and bare soil (yellow), and grass (green). Error bars give the standard deviation. (For interpretation of the references to color in this figure legend, the reader is referred to the web version of this article.)

For all wells, heat input from sand covered areas and green spaces show the highest relative annual variation of >100% throughout the years. Heat input from asphalt has the same absolute variation (~0.5 MJ/m^2 for the mean heat input of all wells). However, it is higher in absolute value and has a higher uncertainty, making it a more stable source of anthropogenic heat input into the underground than the other land cover types. Heat input from buildings varies the least with differences of only 0.05 MJ/m^2 between years. This implies that buildings are the most reliable source for the shallow geothermal potential and shallow geothermal heat pumps applied in urban areas essentially perform heat recycling. Overall, the two most dominant sources of heat input, buildings and asphalt, are also the most stable sources of heat input and for most wells variation between years is less than the uncertainty for the individual years. Among the three input parameters changing over time – air temperature, groundwater temperatures and groundwater depth – air temperature has the highest impact on annual heat input. Pearson correlation between mean annual heat input and air temperatures is above 0.9 (p-value <0.001) for all wells (Table S2). There is no correlation found between annual heat input and groundwater temperature or groundwater depth (p-value ≫ 0.2).

3.3. Cumulative anthropogenic heat input and increase in heat storage

Results for the cumulative heat input (Eq. (3)) and the increase in heat storage (Eq. (4)) are provided in Fig. 5 and Table S1. The difference between median heat input and median increase in heat storage ranges from 33 MJ/m^2 in wells #4 and #30 to −25 MJ/m^2 in well #25; both parameters do not correlate (correlation coefficient: −0.2; p-value: 0.4). In general, the modeled heat input from anthropogenic sources is higher than the observed increase in heat storage for eleven out of the 15 analyzed observation wells. However, for the four wells where the determined heat input is lower than heat storage increase, additional heat sources or anomalies not considered in our model could be identified:

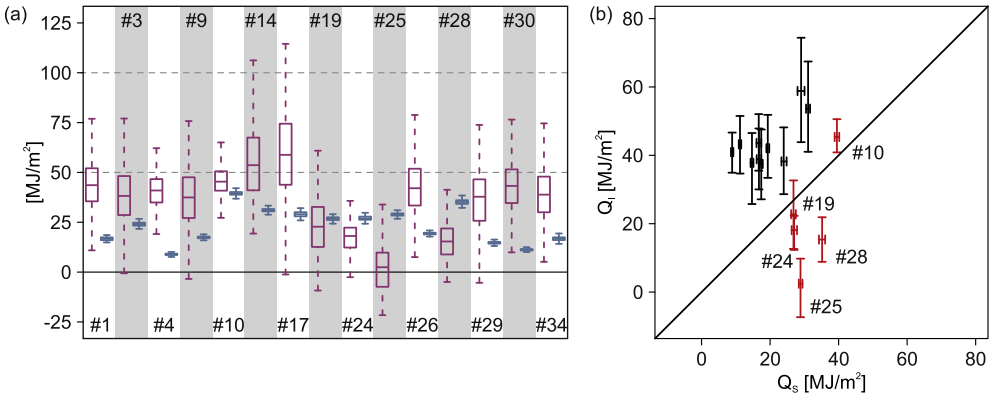

Fig. 5. Relationship between cumulative heat input from anthropogenic sources (Q_l in purple, Eq. (3)) and increase in heat storage (Q_S in blue, Eq. (4)) during the 8 years from 2003 to 2011. (a) As in Fig. 4 the black lines in the boxplot indicate median values, the bars correspond to the inner quartile range (IQR) ranging from the 25th percentile (p_{25}) to the 75th percentile (p_{75}). Whiskers span from the lowest value higher than $p_{25} - 1.5 \cdot IQR$ to the highest value lower than $p_{75} + 1.5 \cdot IQR$. (b) Direct comparison between heat storage (x-axis) and heat input (y-axis). Shown are median values and interquartile ranges. Wells for which additional heat sources could be identified are marked in red. (For interpretation of the references to color in this figure legend, the reader is referred to the web version of this article.)

Well #19 (mean heat input: 22.9 ± 13.6 MJ/m^2; mean increase in heat storage: 26.8 ± 0.9 MJ/m^2) is located a little >100 m west of the Osaka Pool, which has a large underground parking garage. As groundwater is generally flowing westwards at this location, the parking garage is expected to influence groundwater temperatures at the well. Numerical simulations of conditions beneath Basel, Switzerland and Paris, France, found temperature anomalies caused by underground structures in the saturated zone to reach up to several 100 m downstream (Attard et al., 2016; Epting et al., 2017).

Well #24 (mean heat input: 15.1 ± 11.2 MJ/m^2; mean increase in heat storage: 27.1 ± 1.1 MJ/m^2) is positioned in Ohama park on top of a small artificial hill with an elevation of approximately 2–3 m. Thus, most heat sources surrounding this well, mainly all paved areas and most buildings, are at a lower elevation than the top of the well and <20 m above our reference depth. Accordingly, the real thermal gradient and therefore heat fluxes and input are most probably higher than what the 1D model predicts.

Well #28 (mean heat input: 15.4 ± 9.6 MJ/m^2; mean increase in heat storage: 35.2 ± 1.2 MJ/m^2) is located on the property of a waste water treatment plant, which uses an activated sludge process. Such processes are operated at a temperature between 30 and 38 °C or 49–57 °C (Qasim, 1999), and represent an additional local heat source for groundwater.

As discussed before, areas close to well #25 (mean heat input: 3.6 ± 18.0 MJ/m^2; mean increase in heat storage: 28.9 ± 0.8 MJ/m^2) were undergoing major construction work that started in 2007, including the construction of several temporary warehouses. It was only completed in 2014 three years after the here analyzed timeframe. While this work was implemented in our model as a land cover change, comparison to heat input indicates that the construction work had a much more extensive impact on groundwater temperatures than only the associated land cover changes. Because groundwater temperatures in well #25 were also measured in 1999, we were able to additionally quantify the heat input and heat storage increase between 1999 and 2003 for this well. During this time, there was no construction work and heat input and heat storage increase compare much better (mean heat input: 3.9 ± 8.3 MJ/m^2; mean increase in heat storage: 7.4 ± 0.4 MJ/m^2) (Fig. S5). However, heat storage increase is still underestimated, indicating that additional fluxes might be present or that our method overestimates the cooling effect of green areas. Well #25 is the only location, where it is neither asphalt nor buildings but grass cover that is dominant. As surface temperature estimates in this study are based on measurements in Prague, Czech Republic, we cannot rule out that, for example, vegetation in Osaka, Japan, has a different impact on temperatures.

Minor construction work was also observed close to well #10. While heat input (45.7 ± 7.9 MJ/m^2) and increase in heat storage (39.5 ± 1.0 MJ/m^2) agree quite well, it is likely that the impact of the construction work is still present. For all other wells without an additional heat source nearby, the predicted heat input is significantly higher than heat storage increase. Hence, we have to consider that the underestimation of the construction work near well #10 and the discrepancies between heat input and heat accumulation, as observed in all other wells, just cancel each other out. In general, it appears that not all of the anthropogenic heat input into the subsurface is stored there.

When all five wells, for which additional heat sources could be identified, are discounted, correlation between modeled heat input and increase in heat storage becomes reasonable with 0.7 (p-value: 0.03), but predicted heat input is 14 to 33 MJ/m^2 higher than heat storage increase. The most likely hypothesis for this is horizontal heat transport by advection. A recent study by Mueller et al. (2018) in Basel used a 3D heat flow model and predicted significantly more heat output than input at a river boundary. Accordingly in this study well #4, located at the natural shore of the Ina River, has the highest discrepancies and mean heat input is >450% of mean heat storage increase. Similar, Attard et al. (2016) found that only 40% of the heat loss from underground structures is stored in the aquifer. Because the discrepancies between heat input and increase in heat storage cannot be linked to the presence of a specific heat source (e.g. high building density), a significant error in one of the input parameters such as building temperatures, which would impact fluxes from different heat sources differently, is unlikely. Still, we must note that a general overestimation of temperatures at the surface and in buildings is possible. While substantial uncertainties in governing parameter values are accounted for within the presented Monte Carlo analysis, additional effects, such as shadowing at the surface, differences between room temperature and floor temperature in buildings, or latent heat transport in soil, are not considered. Additionally, it should be noted that only 10 wells are analyzed here and groundwater profiles were taken 8 years apart. This space and time resolution is not sufficient for exhaustive characterization of the conditions beneath a city such as Osaka.

4. Conclusions

Both the anthropogenic heat input and the increase in heat storage of the urban aquifer in Osaka are quantified. By means of 15 boreholes, heat fluxes from the surface to a reference depth of 20 m were determined for buildings and for different land cover types (asphalt, sand and bare soil, and grass) using a statistical analytical 1D heat flux

model with a Monte Carlo approach. This analysis was completed for each year between 2003 and 2011 individually, giving the temporal evolution of heat fluxes in an urban setting.

We found that in the absence of underground structures and basements, asphalt covered land causes heat fluxes of a similar magnitude as buildings with 0.28 ± 0.07 W/m^2 and 0.32 ± 0.18 W/m^2, respectively. These numbers are considerably smaller than fluxes that were previously determined for European cities (>0.3 W/m^2 for fluxes from the surface and > 0.5 W/m^2 for fluxes from buildings; Benz et al., 2015; Menberg et al., 2013b; Mueller et al., 2018) due to the lower thermal gradient and lack of basements in Osaka, Japan. In contrast, fluxes from green areas are predicted to be mainly below zero and therefore represent areas of heat release from the ground.

On average, the combined annual heat input of all considered heat sources is lowest in 2006 and 2008 with 4.0 MJ/m^2 and highest in 2003 with 5.9 MJ/m^2. However, temporal variations are small compared to the associated uncertainty. This is because temporal variations are associated with fluctuations of air temperature, and the dominant heat flux (from buildings) is the most stable. Additionally, observed land cover changes near two wells are predicted to have only minor impact on annual heat input. However, comparison with observed heat storage increase indicates that associated construction work, which is not covered by the model, has caused growing groundwater temperatures. Overall simulated heat input is not sufficient to justify the observed increase of groundwater temperatures for about one third of all wells. Here, additional heat sources, such as underground structures in close surroundings, exist. This indicates strongly that small scale, detailed analysis is necessary when discussing urban groundwater temperatures and their sustainable geothermal potential. If wells with additional heat sources are not considered, correlation between estimated heat input and increase in heat storage is reasonable at 0.7.

However, our model predicts heat input to be significantly higher than heat storage increase for all these wells. Based on our analysis, it appears that a significant percentage of anthropogenic heat flux is not stored within the subsurface urban heat island, but transported elsewhere such as to nearby surface waters. However, even a more precise full 3D model would hardly predict a substantially lower heat input without additional, more precise data. Overall, a much more detailed monitoring of input parameters, such as surface and floor temperatures, as well as of temperatures in the surrounding groundwater and surface water is crucial to answer remaining questions about conductive and also advective heat fluxes in urban aquifers.

Still, establishing this connection between anthropogenic heat input and groundwater temperatures is a major step in the development of a sustainable and reliable energy management and heat recycling in urban areas using shallow geothermal systems. Future studies might also use this connection in combination with the link between groundwater temperatures and satellite derived land surface temperatures previously described in Benz et al. (2017a) to develop goundwater temperature forecast systems.

Acknowledgements

We want to thank the Japan Society for the Promotion of Science (JSPS) for supporting S. Benz as an International Research Fellow, and the German Research Foundation (DFG) for supporting P. Bayer (BA2850/3-1). Furthermore, Osaka prefecture and Osaka city are gratefully acknowledged for maintaining the boreholes. We also want to thank three anonymous reviewers and Barret Kurylyk for their helpful and constructive comments.

Appendix A

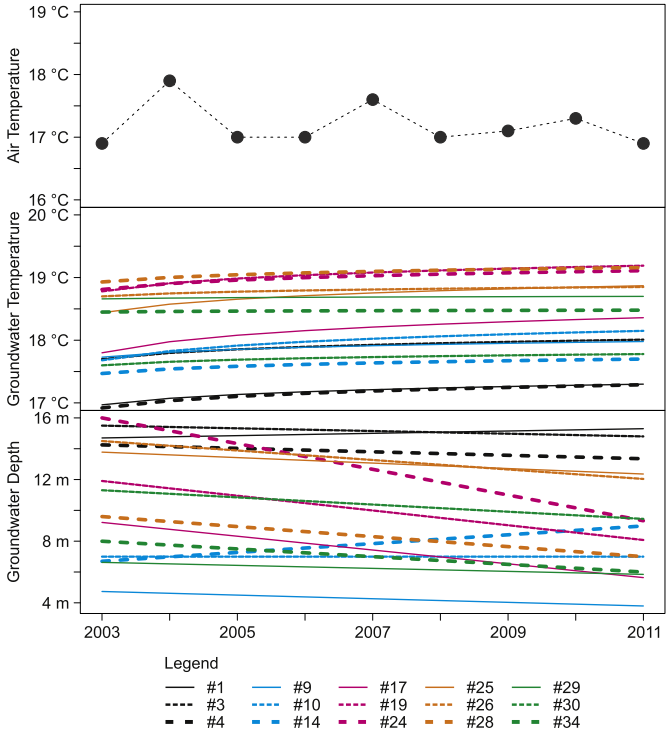

Fig. A1. Groundwater temperature, air temperature and groundwater depth in the analyzed time window 2003 to 2011. Measurements in the groundwater were taken in 2003 and 2011.

Table A1
Results for multi annual mean heat flux q_j^i for all individual heat sources (Eq. (1)), cumulative heat input Q_I (Eq. (3)) and increase in heat storage Q_S (Eq. (4)). Given are mean values and standard deviation.

Well ID	Heat flux [W/m^2] from				Heat input [MJ/m^2]	Heat storage [MJ/m^2]
	buildings	asphalt	sand	grass		
#1	0.34 ± 0.15	0.31 ± 0.04	0.12 ± 0.03	0.04 ± 0.03	43.7 ± 13.5	16.7 ± 0.8
#3	0.30 ± 0.15	0.26 ± 0.04	0.07 ± 0.03	−0.01 ± 0.02	38.3 ± 15.4	24.0 ± 1.0
#4	0.35 ± 0.15	0.32 ± 0.04	0.13 ± 0.03	0.04 ± 0.03	41.6 ± 10.7	8.9 ± 0.5
#9	0.38 ± 0.19	0.33 ± 0.06	0.10 ± 0.03	−0.01 ± 0.03	36.7 ± 15.8	17.4 ± 0.6
#10	0.38 ± 0.19	0.33 ± 0.05	0.09 ± 0.03	−0.02 ± 0.03	45.7 ± 7.9	39.5 ± 1.0
#14	0.40 ± 0.19	0.35 ± 0.05	0.12 ± 0.03	0.01 ± 0.03	55.0 ± 18.2	31.1 ± 0.8
#17	0.37 ± 0.20	0.32 ± 0.04	0.08 ± 0.03	−0.04 ± 0.04	59.6 ± 22.7	29.0 ± 1.3
#19	0.26 ± 0.17	0.21 ± 0.04	0.00 ± 0.03	−0.10 ± 0.03	22.9 ± 13.6	26.8 ± 0.9
#24	0.25 ± 0.16	0.20 ± 0.04	0.00 ± 0.03	−0.09 ± 0.03	15.1 ± 11.2	27.1 ± 1.1
#25	0.28 ± 0.17	0.24 ± 0.04	0.02 ± 0.03	−0.08 ± 0.03	3.6 ± 18.0	28.9 ± 0.8
#26	0.25 ± 0.16	0.21 ± 0.04	0.01 ± 0.02	−0.08 ± 0.03	44.3 ± 16.7	19.3 ± 0.6
#28	0.26 ± 0.17	0.21 ± 0.03	−0.01 ± 0.03	−0.11 ± 0.03	15.4 ± 9.6	35.2 ± 1.2
#29	0.30 ± 0.18	0.25 ± 0.04	0.02 ± 0.03	−0.08 ± 0.03	35.5 ± 17.4	14.7 ± 0.6
#30	0.34 ± 0.16	0.30 ± 0.04	0.10 ± 0.03	0.00 ± 0.03	44.1 ± 14.6	11.2 ± 0.5
#34	0.34 ± 0.19	0.29 ± 0.04	0.05 ± 0.03	−0.07 ± 0.03	39.9 ± 13.9	16.7 ± 0.9
Mean	0.32 ± 0.18	0.28 ± 0.07	0.06 ± 0.06	−0.04 ± 0.06	36.1 ± 21.2	23.1 ± 8.7

Appendix B. Supplementary material

Supplementary data to this article can be found online at https://doi.org/10.1016/j.scitotenv.2018.06.253.

References

Allen, A., Milenic, D., Sikora, P., 2003. Shallow gravel aquifers and the urban 'heat island' effect: a source of low enthalpy geothermal energy. Geothermics 32 (4–6), 569–578.

Arimoto, H., Taniguchi, M., Hamamoto, H., Kishimoto, Y., Mizuma, K., Kobayashi, N., 2015. Subsurface warming in the Osaka plain. Proceedings of the Kansai Geo-Symposium 2015. Kansai Branch of Japanese Geotechnical Society, pp. 71–76.

Arnfield, A.J., 2003. Two decades of urban climate research: a review of turbulence, exchanges of energy and water, and the urban heat island. Int. J. Climatol. 23 (1), 1–26.

Arola, T., Korkka-Niemi, K., 2014. The effect of urban heat islands on geothermal potential: examples from Quaternary aquifers in Finland. Hydrogeol. J. 22 (8), 1953–1967.

Attard, G., Rossier, Y., Winiarski, T., Eisenlohr, L., 2016. Deterministic modeling of the impact of underground structures on urban groundwater temperature. Sci. Total Environ. 572, 986–994.

Bayer, P., Saner, D., Bolay, S., Rybach, L., Blum, P., 2012. Greenhouse gas emission savings of ground source heat pump systems in Europe: a review. Renew. Sust. Energ. Rev. 16 (2), 1256–1267.

Bayer, P., Rivera, J.A., Schweizer, D., Schärli, U., Blum, P., Rybach, L., 2016. Extracting past atmospheric warming and urban heating effects from borehole temperature profiles. Geothermics 64, 289–299.

Bense, V.F., Kurylyk, B.L., 2017. Tracking the subsurface signal of decadal climate warming to quantify vertical groundwater flow rates. Geophys. Res. Lett. 44 (24), 12,244–12,253.

Bense, V.F., Kurylyk, B.L., van Daal, J., van der Ploeg, M.J., Carey, S.K., 2017. Interpreting repeated temperature-depth profiles for groundwater flow. Water Resour. Res. 53 (10), 8639–8647.

Benz, S.A., Bayer, P., Menberg, K., Jung, S., Blum, P., 2015. Spatial resolution of anthropogenic heat fluxes into urban aquifers. Sci. Total Environ. 524-525, 427–439.

Benz, S.A., Bayer, P., Goettsche, F.M., Olesen, F.S., Blum, P., 2016. Linking surface urban heat islands with groundwater temperatures. Environ. Sci. Technol. 50 (1), 70–78.

Benz, S.A., Bayer, P., Blum, P., 2017a. Global patterns of shallow groundwater temperatures. Environ. Res. Lett. 12 (3), 34005.

Benz, S.A., Bayer, P., Blum, P., 2017b. Identifying anthropogenic anomalies in air, surface and groundwater temperatures in Germany. Sci. Total Environ. 584-585, 145–153.

Bodri, L., Cermak, V., 2011. Borehole Climatology: A New Method How to Reconstruct Climate. Elsevier Science, Burlington.

Bucci, A., Barbero, D., Lasagna, M., Forno, M.G., de Luca, D.A., 2017. Shallow groundwater temperature in the Turin area (NW Italy): vertical distribution and anthropogenic effects. Environ. Earth Sci. 76 (5), 569.

Cermak, V., Bodri, L., Kresl, M., Dědeček, P., Šafanda, J., 2017. Eleven years of ground-air temperature tracking over different land cover types. Int. J. Climatol. 37 (2), 1084–1099.

Colombani, N., Giambastiani, B.M.S., Mastrocicco, M., 2016. Use of shallow groundwater temperature profiles to infer climate and land use change: interpretation and measurement challenges. Hydrol. Process. 30 (14), 2512–2524.

Dědeček, P., Šafanda, J., Rajver, D., 2012. Detection and quantification of local anthropogenic and regional climatic transient signals in temperature logs from Czechia and Slovenia. Clim. Chang. 113 (3–4), 787–801.

Dettwiller, J., 1970. Deep soil temperature trends and urban effects at Paris. J. Appl. Meteorol. 9 (1), 178–180.

Energy consumption in households: final energy consumption in the residential sector by type of end-use. EU-28, p. 2015.

Epting, J., Huggenberger, P., 2013. Unraveling the heat island effect observed in urban groundwater bodies – definition of a potential natural state. J. Hydrol. 501, 193–204.

Epting, J., Scheidler, S., Affolter, A., Borer, P., Mueller, M.H., Egli, L., et al., 2017. The thermal impact of subsurface building structures on urban groundwater resources - a paradigmatic example. Sci. Total Environ. 596-597, 87–96.

Ewing, R., Rong, F., 2008. The impact of urban form on U.S. residential energy use. Housing Policy Debate 19 (1), 1–30.

Farr, G.J., Patton, A.M., Boon, D.P., James, D.R., Williams, B., Schofield, D.I., 2017. Mapping shallow urban groundwater temperatures, a case study from Cardiff, UK. Q. J. Eng. Geol. Hydrogeol. 50 (2), 187–198.

Ferguson, G., Woodbury, A.D., 2004. Subsurface heat flow in an urban environment. J. Geophys. Res. 109 (B2), 327.

Ferguson, G., Woodbury, A.D., 2007. Urban heat island in the subsurface. Geophys. Res. Lett. 34 (23), L23713.

García-Gil, A., Vázquez-Suñe, E., Schneider, E.G., Sánchez-Navarro, J.Á., Mateo-Lázaro, J., 2014. The thermal consequences of river-level variations in an urban groundwater body highly affected by groundwater heat pumps. Sci. Total Environ. 485-486, 575–587.

Goto, S., Hamamoto, H., Yamano, M., 2005. Climatic and environmental changes at southeastern coast of Lake Biwa over past 3000 years, inferred from borehole temperature data. Phys. Earth Planet. Inter. 152 (4), 314–325.

Hasegawa, 2013. Introduction to the Building Standard Law - Building Regulations in Japan. https://www.bcj.or.jp/en/services/reference.html.

Herb, W.R., Janke, B., Mohseni, O., Stefan, H.G., 2008. Ground surface temperature simulation for different land covers. J. Hydrol. 356 (3–4), 327–343.

Herbert, A., Arthur, S., Chillingworth, G., 2013. Thermal modelling of large scale exploitation of ground source energy in urban aquifers as a resource management tool. Appl. Energy 109, 94–103.

Huang, S., Taniguchi, M., Yamano, M., Wang, C.-H., 2009. Detecting urbanization effects on surface and subsurface thermal environment–a case study of Osaka. Sci. Total Environ. 407 (9), 3142–3152.

Ichinose, T., Shimodozono, K., Hanaki, K., 1999. Impact of anthropogenic heat on urban climate in Tokyo. Atmos. Environ. 33 (24–25), 3897–3909.

Japan Meteorological Agency, d. Monthly mean air temperature (°C) - OSAKA WMO Station ID: 47772http://www.data.jma.go.jp/obd/stats/etrn/view/monthly_s3_en.php?block_no=47772&view=1 (accessed January 31, 2018).

Japan Ministry of Land, d. Infrastructure, Transport and Tourism, Land and Water Bureau, National Land Survey Division. 近畿地域地下水マップ大阪・兵庫(その2) (The hydrological map of the Kinki area: Osaka and Hyogo (Part 2))http://nrb-www.mlit.go.jp/kokjo/tochimizu/F8/MAP/810002.jpg (accessed June 15, 2018).

Kansai Geo-informatic Network (KG-NET), 2007. 新関西地盤-大阪平野から大阪湾 (The foundation of the Kansai area from the Osaka Plain to Osaka Bay). Osaka.

Kolokotroni, M., Giannitsaris, I., Watkins, R., 2006. The effect of the London urban heat island on building summer cooling demand and night ventilation strategies. Sol. Energy 80 (4), 383–392.

Komiyama, R., Marnay, C., 2008. Japan's Residential Energy Demand Outlook to 2030 Considering Energy Efficiency Standards "Top-Runner Approach".

Kooi, H., 2008. Spatial variability in subsurface warming over the last three decades; insight from repeated borehole temperature measurements in The Netherlands. Earth Planet. Sci. Lett. 270 (1–2), 86–94.

Kurylyk, B.L., MacQuarrie, K.T.B., 2014. A new analytical solution for assessing climate change impacts on subsurface temperature. Hydrol. Process. 28 (7), 3161–3172.

Kurylyk, B.L., MacQuarrie, K.T.B., McKenzie, J.M., 2014. Climate change impacts on groundwater and soil temperatures in cold and temperate regions: implications, mathematical theory, and emerging simulation tools. Earth Sci. Rev. 138, 313–334.

Menberg, K., Bayer, P., Zosseder, K., Rumohr, S., Blum, P., 2013a. Subsurface urban heat islands in German cities. Sci. Total Environ. 442, 123–133.

Menberg, K., Blum, P., Schaffitel, A., Bayer, P., 2013b. Long-term evolution of anthropogenic heat fluxes into a subsurface urban heat island. Environ. Sci. Technol. 47 (17), 9747–9755.
Ministry of Health, Labor and Welfare, Japan, d. The management standard of environmental sanitation for buildingshttp://www.mhlw.go.jp/bunya/kenkou/seikatsu-eisei10/ (accessed January 31, 2018).
Mitamura, M., Matsuyama, M., Nakagawa, K., Yamamoto, K., Suwa, S., 1994. Stratigraphy and subsurface structure of Holocene Deposits around Uemachi Upland in the Central Osaka Plain. J. Geosci. Osaka City Univ. (37), 183–212.
Mueller, M.H., Huggenberger, P., Epting, J., 2018. Combining monitoring and modelling tools as a basis for city-scale concepts for a sustainable thermal management of urban groundwater resources. Sci. Total Environ. 627, 1121–1136.
Müller, N., Kuttler, W., Barlag, A.B., 2014. Analysis of the subsurface urban heat island in Oberhausen, Germany. Clim. Res. 58 (3), 247–256.
Oke, T.R., 1973. City size and the urban heat island. Atmos. Environ. (1967) 7 (8), 769–779.
Patz, J.A., Campbell-Lendrum, D., Holloway, T., Foley, J.A., 2005. Impact of regional climate change on human health. Nature 438 (7066), 310–317.
Peel, M.C., Finlayson, B.L., McMahon, T.A., 2007. Updated world map of the Köppen-Geiger climate classification. Hydrol. Earth Syst. Sci. Discuss. 4 (2), 439–473.
Qasim, S.R., 1999. Wastewater Treatment Plants: Planning, Design, and Operation. 2nd ed. CRC Press, Boca Raton.
Raghavan, S.V., Wei, M., Kammen, D.M., 2017. Scenarios to decarbonize residential water heating in California. Energy Policy 109, 441–451.
Reiter, M., 2006. Vadose zone temperature measurements at a site in the northern Albuquerque Basin indicate ground-surface warming due to urbanization. Environ. Eng. Geosci. 12 (4), 353–360.
Rivera, J.A., Blum, P., Bayer, P., 2017. Increased ground temperatures in urban areas: estimation of the technical geothermal potential. Renew. Energy 103, 388–400.
Šafanda, J., Rajver, D., Correia, A., Dědeček, P., 2007. Repeated temperature logs from Czech, Slovenian and Portuguese borehole climate observatories. Clim. Past 3 (3), 453–462.
Santamouris, M., 2014. On the energy impact of urban heat island and global warming on buildings. Energ. Buildings 82, 100–113.
Sivak, M., 2009. Potential energy demand for cooling in the 50 largest metropolitan areas of the world: implications for developing countries. Energy Policy 37 (4), 1382–1384.
Taniguchi, M., Uemura, T., 2005. Effects of urbanization and groundwater flow on the subsurface temperature in Osaka, Japan. Phys. Earth Planet. Inter. 152 (4), 305–313.
Taniguchi, M., Uemura, T., Jago-on, K., 2007. Combined effects of urbanization and global warming on subsurface temperature in four Asian cities. Vadose Zone J. 6 (3), 591.
Taniguchi, M., Shimada, J., Fukuda, Y., Yamano, M., Onodera, S.-i., Kaneko, S., et al., 2009. Anthropogenic effects on the subsurface thermal and groundwater environments in Osaka, Japan and Bangkok, Thailand. Sci. Total Environ. 407 (9), 3153–3164.
U.S. Energy Information Administration (EIA), 2012. Residential Energy Consumption Survey (RECS): Household Site End-Use Consumption in the U.S., Totals and Averages, 2009. https://www.eia.gov/consumption/residential/data/2009/.
United Nations, Department of Economic and Social Affairs, Population Division, 2015. World Urbanization Prospects: The 2014 Revision. ST/ESA/SER.A/366.
Vandentorren, S., Bretin, P., Zeghnoun, A., Mandereau-Bruno, L., Croisier, A., Cochet, C., et al., 2006. August 2003 heat wave in France: risk factors for death of elderly people living at home. Eur. J. Pub. Health 16 (6), 583–591.
Verein Deutscher Ingenieure (VDI), 2010. Thermische Nutzung des Untergrunds: Grundlagen, Genehmigungen, Umweltaspekte (Thermal use of the underground: Fundamentals, approvals, environmental aspects). VDI 4640. Beuth Verlag GmbH, Berlin.
Westaway, R., Scotney, P.M., Younger, P.L., Boyce, A.J., 2015. Subsurface absorption of anthropogenic warming of the land surface: the case of the world's largest brickworks (Stewartby, Bedfordshire, UK). Sci. Total Environ. 508, 585–603.
Yalcin, T., Yetemen, O., 2009. Local warming of groundwaters caused by the urban heat island effect in Istanbul, Turkey. Hydrogeol. J. 17 (5), 1247–1255.
Yamano, M., Goto, S., Miyakoshi, A., Hamamoto, H., Lubis, R.F., Monyrath, V., et al., 2009. Reconstruction of the thermal environment evolution in urban areas from underground temperature distribution. Sci. Total Environ. 407 (9), 3120–3128.
Zhu, K., Blum, P., Ferguson, G., Balke, K.-D., Bayer, P., 2010. The geothermal potential of urban heat islands. Environ. Res. Lett. 5 (4), 44002.